IOPscience iopscience.iop.org

Home Search Collections Journals About Contact us My IOPscience

Frequency response of mesoscopic conductors: a time-dependent Landauer approach

This article has been downloaded from IOPscience. Please scroll down to see the full text article.

1994 J. Phys.: Condens. Matter 6 5061

(http://iopscience.iop.org/0953-8984/6/27/015)

View the table of contents for this issue, or go to the journal homepage for more

Download details:
IP Address: 171.66.16.147
The article was downloaded on 12/05/2010 at 18:47

Please note that terms and conditions apply.

J. Phys.: Condens. Matter 6 (1994) 5061–5068. Printed in the UK

Frequency response of mesoscopic conductors: a time-dependent Landauer approach

L Y Chen and S C Ying
Department of Physics, Brown University, Providence, RI 02912, USA

Received 21 March 1994, in final form 4 May 1994

Abstract. We employ a time-dependent Landauer approach to study the dynamic response of a mesoscopic conductor biased with a temporal varying voltage. The system is modelled as a perfect conducting wire coupled to two large electron reservoirs whose chemical potentials are driven offset by the bias. The electronic waves are quantized on the basis of orthonormal wave packets moving along the conductor. The time for an electron to traverse the wire between the source and the drain reservoirs is found to be the relevant time scale in determining the transient response and the characteristic frequency of the AC conductance.

1. Introduction

Electronic transport in mesoscopic systems is a field of increasing interest for its fundamental importance as well as for its potential technological applications [1, 2]. The quantum nature of this problem has been successfully described by the Landauer approach [1, 3] for two probe systems and the Büttiker–Landauer approach [4] for multi-probe systems. An elegant example is the ballistic transport through a two-dimensional point contact system: its conductance was found to be quantized at multiples of a fundamental constant e^2/h [5, 6]. While the DC characteristics of various mesoscopic systems are well understood, investigation of dynamic properties has been limited to systems such as double-barrier resonant-tunnelling structures [7]. In these systems, the energy scale $\Delta\epsilon$ over which the transmission coefficient $|T|^2$ varies significantly determines the characteristic frequency and the transient time [8–14] since the time scale $\tau = \hbar/\Delta\epsilon$ is the longest among all the relevant time scales. When the frequency of an AC bias is greater than $2\pi/\tau$, the system becomes unable to respond instantaneously and consequently the conductance falls below its DC level. In a recent paper, Büttiker *et al* [15] investigated the AC admittance of general mesoscopic conductors and found that energy dependence of the phase shift in the scattering matrix gives a relevant time scale for the frequency response. In a perfect conductor, however, the conducting channel can be completely open and the transmission coefficient is energy independent. Therefore the aforementioned time scale as determined by the energy dependence of the scattering matrix is irrelevant. One can then ask the question of what is the new relevant transient time scale, or, at what frequency does the AC conductance start to deviate seriously from its DC limit. In this paper, we answer this question and provide a derivation of the frequency dependent conductance as well as the imaginary part of the admittance. The method we employ is a time-dependent Landauer approach. As will be illustrated in the following discussion, the relevant time scale is determined by the time for an electron to traverse the conducting channel from the source reservoir to the drain, namely,

0953-8984/94/275061+08$19.50 © 1994 IOP Publishing Ltd

$\tau_0 = L/v_g$ where v_g is the group velocity of an electron wave packet in the channel. With increasing frequency Ω of the applied bias voltage, the response current decreases and its spatial variation at length scale of $l_\Omega = v_g/\Omega$ also becomes observable at high frequencies.

2. Time-dependent wave packet formalism

In the Landauer approach, a mesoscopic conductor is pictured as an elastic scatterer and thus the scattering wave functions are of essential importance [16]. The system we study in this work can be characterized by a Hamiltonian consisting of the kinetic energy plus the geometric confinement potential energy which divides the electron gas into two 2D regions (reservoirs) and a one-dimensional channel. Here we choose the coordinates with the x axis along the channel and the y axis perpendicular to it. In the adiabatic approximation [17], the incident waves on the channel are either completely transmitted or completely reflected. A wave, $\phi_p^L(x, y)$, incident from the left and completely reflected extends only in the left reservoir region and a wave $\phi_p^R(x, y)$ incident from the right and completely reflected exists in the right reservoir. In addition to these two sets of reservoir states, there exist channel states including waves incident from the left or right and completely transmitted to the other side which extend throughout the channel region from one reservoir to the other. The coherence length of a channel state is determined by scattering within the reservoirs as well as by its coupling to the reservoirs. Its value is obviously system dependent and can be experimentally tuned. Starting from the extended channel states in the adiabatic approximation, we construct orthonormal wave packet states $\bar{\phi}_{k,x_0}(x, y)$ of the form

$$\bar{\phi}_{k,x_0}(x, y) = \phi(y; x_0)\phi_{k,x_0}(x). \tag{2.1}$$

Here $\phi(y; x_0)$ is the lateral wave function [17]

$$\phi(y; x_0) = \frac{1}{\sqrt{d(x_0)}} \sin\left(\frac{\pi[y - d(x_0)]}{2d(x_0)}\right). \tag{2.2}$$

where $2d(x)$ is the width of the channel at position x. The wave packet along the x direction is defined as

$$\phi_{k,x_0}(x) = e^{i\bar{k}(x-x_0)} \frac{1}{\sqrt{NL_0}} \sum_{q=-\sigma/2}^{\sigma/2} e^{iq(x-x_0)} \equiv \phi_k(x - x_0) \tag{2.3}$$

which is centred at x_0 with a width $\xi = 2\pi/\sigma$. (Here L_0 is the size of the entire system and $N = \sigma L_0/2\pi$.) The average momentum $\bar{k}(k, x_0)$ is a function of the position of the centre of the wave packet defined as

$$\frac{2m}{\hbar^2}\epsilon_k = \bar{k}^2(k, x_0) + \left(\frac{\pi}{2d(x_0)}\right)^2 = k^2 + \left(\frac{\pi}{2d_0}\right)^2. \tag{2.4}$$

In equation (2.4), $\hbar k$ is the average of the momentum at the centre of the channel (x=0). The wave packet thus constructed forms an orthonormal set if we choose $\bar{k}$ to be multiples of σ ($\bar{k} \gg \sigma$) and x_0 to be multiples of ξ. We use the complete set of wave functions $\phi_p^L(x, y)$, $\phi_p^R(x, y)$ and $\bar{\phi}_{k,x_0}(x, y)$ to perform the second quantization of electron waves. The electron field operators

$$\psi(x, y) = \sum_k \sum_{x_0} c_{kx_0}\bar{\phi}_{kx_0}(x, y) + \sum_p a_p\phi_p^L(x, y) + \sum_p b_p\phi_p^R(x, y) \tag{2.5}$$

and its Hermitian conjugate $\psi^\dagger(x, y)$ satisfy the canonical anti-commutation relations and c_{kx_0} and $c^\dagger_{kx_0}$ are respectively the canonical fermionic annihilation and creation operators on the state $\phi_{kx_0}(x)$. Obviously, there exist couplings between the channel states (the scattering wave packets) and the reservoir states by for example impurities in reservoir regions adjacent to the channel. This coupling can be modelled in a simple transfer matrix form. Then the Hamiltonian of the system can be written as

$$H = H_D + \sum_k \sum_{x_0} \left(\epsilon_k c^\dagger_{kx_0} c_{kx_0} + \sum_p T_1(k, x_0; p) c^\dagger_{kx_0} a_p + T_1^*(k, x_0; p) a^\dagger_p c_{kx_0} \right.$$
$$\left. + \sum_p T_2(k, x_0; p) c^\dagger_{kx_0} b_p + T_2^*(k, x_0; p) b^\dagger_p c_{kx_0} \right) + H_1(a, a^\dagger) + H_2(b, b^\dagger) \tag{2.6}$$

where a term in order of σ^2 has been dropped [18]. The coupling coefficients $T_1(k, x_0; p)$ and $T_2(k, x_0; p)$ are respectively determined by the overlap between $\phi_{kx_0}(x)$ and the reservoir electron wave functions. $a, a^\dagger$ and $b, b^\dagger$ are respectively the annihilation, creation operators of electrons in the two reservoirs with Hamiltonians H_1 and H_2. The drifting part of the Hamiltonian

$$H_D = \sum_k \sum_{x_0} \frac{\hbar \bar{k}}{m} c^\dagger_{kx_0} \left(-i \frac{\hbar \partial}{\partial x_0} \right) c_{kx_0} \tag{2.7}$$

drives the particles on the wave packets $\bar{\phi}_{kx_0}$ states with momentum $\hbar\bar{k} > 0$ moving to the right and those with $\hbar\bar{k} < 0$ moving to the left. It is convenient to transform into the interaction representation of H_D, resulting in an effective Hamiltonian H_{eff}

$$H_{\text{eff}} = \sum_k \sum_{x_0} \left(\epsilon_k c^\dagger_{kx_0} c_{kx_0} + \sum_p T_1(t) c^\dagger_{kx_0} a_p + T_1^*(t) a^\dagger_p c_{kx_0} \right.$$
$$\left. + \sum_p T_2(t) c^\dagger_{kx_0} b_p + T_2^*(t) b^\dagger_p c_{kx_0} \right) + H_1(a, a^\dagger) + H_2(b, b^\dagger) \tag{2.8}$$

where $T_1(t) \equiv T_1(k, x_0(t, k); p)$ represents the coupling between the left reservoir and the moving wave packet state $\bar{\phi}_{kx_0}(x, y; t) \equiv \bar{\phi}_{k, x_0(t,k)}(x, y)$ and so does $T_2(t)$ for the coupling to the right reservoir. We have adopted the notation $x_0(t, k)$ for the centre of the wave packet at time t. Note that the time-dependent wave packet state $\phi_{kx_0}(x, y, t) \equiv \phi_k(x - x_0(t, k), y)$ is still characterized by the quantum number x_0 (the position of the centre of wave packet at $t = 0$) and k (average wavevector of the wave packet at the centre of the channel). The description of the system by the Hamiltonian $H_{\text{eff.}}$ is equivalent to choosing time-dependent basis states for the second quantizated operators $c^\dagger_{k,x_0}$ and c_{k,x_0} such that they create and annihilate the time-dependent wave packet state $\phi_{kx_0}(x, y, t)$ respectively. This is the reason why the coupling between the channel state and the reservoirs $T_1(t)$ and $T_2(t)$ depend on time even in the absence of time-dependent biases. Our procedure of arriving at $H_{\text{eff.}}$ through a canonical transformation from the original Hamiltonian H simply gives a rigorous justification for this physically transparent choice.

3. Frequency dependent admittance

When the length of the conductor $L \gg \xi$, the current carried by hopping from one reservoir to the other via a channel state is negligibly small and charges are only transported by the

drifting motion of the wave packets. Namely, the current operator can be written as

$$i(x,t) = \sum_k \sum_{x_0} c^\dagger_{kx_0}(t) c_{kx_0}(t) \frac{e\hbar\bar{k}}{m} |\phi_{kx_0}(x,t)|^2 \tag{3.1}$$

whose quantum statistical average yields the intrinsic current. The time dependence of the creation and annihilation operators here is governed by the effective Hamiltonian H_{eff}. Generally, the measured current, i.e., the circuit current $I(t)$ can be a complicated convolution of $\langle i(x,t)\rangle$ which involves the detailed information of the conductor geometry, the voltage probe contacts and, especially, the capacitance distribution [16]. In what follows we shall concentrate our discussion on the intrinsic part with emphasis on the physics involved.

Due to strong dissipation in the reservoirs, electrons there can be well described by separate equilibrium density matrices with chemical potentials $\mu_1(t)$ and $\mu_2(t)$ respectively which are driven away from the Fermi energy ϵ_F by the applied bias voltage $u(t)$: $\mu_1 = \epsilon_F + eu(t)/2$ and $\mu_2 = \epsilon_F - eu(t)/2$. With the help of the Keldysh formalism of non-equilibrium Green functions [19], the occupation number of the channel state $\overline{\phi}_{kx_0}$ can be found as

$$\begin{aligned} n(k,x_0,t) &= \left\langle c^\dagger_{kx_0}(t) c_{kx_0}(t) \right\rangle \\ &= \int_{-\infty}^{\infty} d\tau\ \theta(t-\tau) \exp\left(-\int_\tau^t du\ \gamma(k,x_0,u)\right) \\ &\quad \times \left[\gamma_1(k,x_0,\tau) f_1(\tau) + \gamma_2(k,x_0,\tau) f_2(\tau)\right]. \end{aligned} \tag{3.2}$$

Here $f_1(t)$ and $f_2(t)$ are the Fermi–Dirac distribution functions with chemical potential $\mu_1(t)$ and $\mu_2(t)$ respectively. $\gamma(k,x_0,t) = \gamma_1(k,x_0,t) + \gamma_2(k,x_0,t)$ and

$$\gamma_{1(2)} = \sum_p |T_{1(2)}(t)|^2 \pi \delta(\epsilon_p - \epsilon_k). \tag{3.3}$$

The detailed evaluation of $\gamma_{1(2)}$ requires a knowledge of the precise geometry of the confining potential for the channel as well as the scattering mechanisms. For our purpose, it is sufficient to replace the channel by a constant width region with an effective length L. The coupling matrix elements γ_1 and γ_2 are characterized by an overall scattering strength γ. We write $\gamma_{1(2)}$ in terms of these two parameters as

$$\gamma_1(k,x_0,t) = \gamma \int_{-\infty}^{-L/2} dx |\phi_{kx_0}(x,t)|^2 = \gamma_1(x_0(t,k)) \tag{3.4}$$

$$\gamma_2(k,x_0,t) = \gamma \int_{L/2}^{\infty} dx |\phi_{kx_0}(x,t)|^2 = \gamma_2(x_0(t,k)). \tag{3.5}$$

Furthermore, we choose γ to be related to the wave packet size in the form $\gamma = \hbar^2 k\sigma/2\pi m$. The final results will be independent of γ as long as $L \gg \xi$. In figure 1, we illustrate the time dependence of $\gamma_{1(2)}$. Note that $\gamma_1(x_0(t,k))$ evolves with time monotonously from γ where $x_0(t,k) \ll -L/2$ to 0 where $x_0(t,k) \gg -L/2$. Moreover, the variation is mainly located around $x_0(t,k) = -L/2$. Similarly, $\gamma_2(x_0(t,k))$ evolves from 0 at $x_0(t,k) \ll L/2$ to γ at $x_0(t,k) \gg L/2$. Consequently, $\gamma(x_0(t,k))$ approximately vanishes inside the wire and takes a constant value γ outside it. On examining the integrand in equation (3.2), we find that the first part peaks at $x_0(\tau,k) = -L/2$ while the second one peaks at $x_0(\tau,k) = L/2$. Therefore the occupation number of the right moving electrons in the channel region

$$n(k,x_0,t) = \int_0^\infty d\tau \exp\left(-\int_\tau^t du\ \gamma(x_0(u,k))\right) \gamma_1(x_0(u,k)) f_1(\tau) \tag{3.6}$$

is only fed by the left (first) reservoir. In equation (3.6) and the following equation (3.7), $k > 0$. The left moving electrons are fed by the right (second) reservoir,

$$n(-k, x_0, t) = \int_0^\infty d\tau \exp\left(-\int_\tau^t du\ \gamma(x_0(u, -k))\right)\gamma_2(x_0(u, -k))f_2(\tau). \tag{3.7}$$

With equations (3.6) and (3.7), the origin of the relevant time of the system becomes transparent. Once an electron (a wave packet) emanates from a reservoir into the channel, it will move ballistically in this dissipationless region with definite velocity ($x_0(t, k) = vt$ with $v = \hbar k/m$) and becomes free from further influence of the dissipative reservoirs until it emerges at the other end. Consequently, the system is unable to respond to an applied bias on a time scale shorter than $\tau_0 = L/v_g$. The group velocity of the wave packet v_g is just the Fermi velocity in the channel.

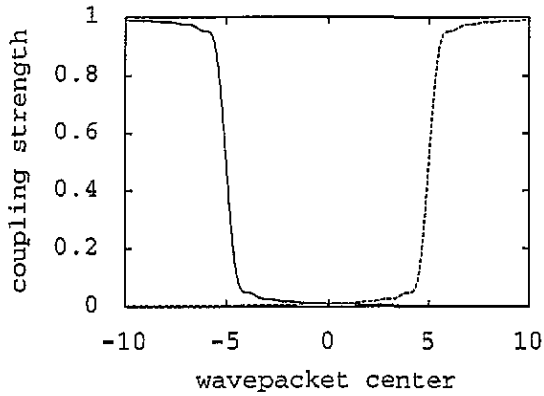

Figure 1. The coupling strength of a wave packet to the reservoirs $\gamma_1(x_0(t, k))$ (solid curve, scaled by γ) and $\gamma_2(x_0(t, k))$ (dashed curve, scaled by γ) versus the centre of the packet $(x_0(t, k))$ (scaled by ξ). The conductor length L=10ξ.

Now we study the frequency dependent admittance of the system subject to an applied AC bias $u(t) = u_0 e^{-i\Omega t}$. At zero frequency $\Omega = 0$, one can show that all the left moving wave packet states are fully occupied while all the right moving ones empty when the left (first) reservoir is biased as the source and the right (second) one as the drain $\mu_1 - \mu_2 = eu_0 > 0$, i.e.,

$$n(k, x_0, t) = 1 \qquad n(-k, x_0, t) = 0 \tag{3.8}$$

where $k > 0$ and $\mu_2 < \epsilon_k < \mu_1$. Then one observes a uniform current throughout conducting wire

$$\langle i(x, t)\rangle = \sum_{k>0}\sum_{x_0} \frac{e\hbar\bar{k}}{m}|\phi_{kx_0}(x, t)|^2 = \int_{\mu_2}^{\mu_1} d\epsilon_k\ \frac{e}{h}|T(\epsilon_k)|^2 \tag{3.9}$$

with the transmission coefficient $|T(\epsilon_k)|^2 = 1$ in this case. Equation (3.9) is the well known Landauer formula which leads to DC conductance $G = e^2/h$ for the single-channel two-probe system we consider here. Generally, $G = ne^2/h$ when n channel state subbands are contributing [5, 6].

When the signal voltage $|u(t)| \ll \epsilon_F/e$, the reservoir distribution functions can be expanded as

$$f_{1(2)}(t) = f_0 + (-)\frac{\partial f_0(\epsilon_k)}{\partial \epsilon_k} eu(t)/2$$

where $f_0(\epsilon_k)$ is the equilibrium Fermi–Dirac distribution function. Furthermore, a coarse graining procedure can be performed over the extension of a wave packet, i.e., we can approximate $\sum_{x_0}$ by $(1/\xi)\int dx_0$ and the current becomes

$$\langle i(x,t)\rangle = g(x,\Omega)u(t)\frac{e^2}{h} \tag{3.10}$$

with relative admittance defined as

$$g(x,\Omega) = \int_{-\infty}^{0} d\tau\, e^{i\Omega\tau}\int_{-\infty}^{\infty} dx_0\, \frac{1}{2}\left[|\phi_{k_F x_0}(x)|^2 + |\phi_{k_F x_0}(-x)|^2\right] \times \exp\left(-\int_0^{\tau} du\gamma(x_0(\tau,-k_F))\right)\gamma_1(x_0(\tau,-k_F)). \tag{3.11}$$

As already discussed above, at zero frequency, $g(x,\Omega=0)=1$ is purely real and uniform throughout the channel region. At a finite frequency Ω comparable to $\Omega_0 = 2\pi v_g/L$, g becomes complex and oscillates with x. These behaviours are illustrated in figure 2. In figure 3, we plot the averaged relative admittance

$$\bar{g}(\Omega) = \frac{1}{L}\int_{-L/2}^{L/2} dx\; g(x,\Omega)$$

versus Ω/Ω_0. As the frequency increases, the system becomes less and less capable of following the change of $u(t)$. This results in the decrease of admittance amplitude and the retardation in response leads to an inductive behaviour as demonstrated by the imaginary part of the admittance. The characteristic frequency Ω_0 typically lies in the range between a few GHz and a few THz. Although directly probing the spatial variance of current within the channel poses considerable challenge, the experimental measurements of the average admittance for frequencies up to several THz are certainly feasible. Similar experiments have actually been carried out for the double barrier structures [9].

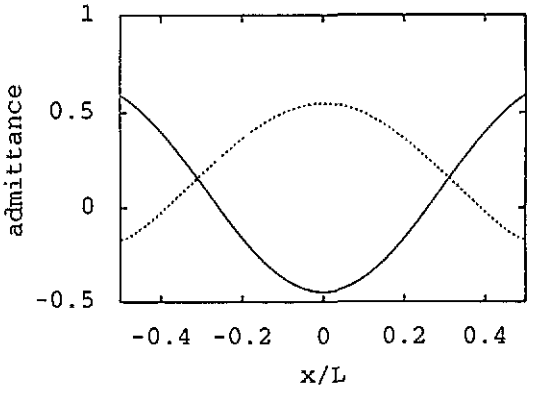

Figure 2. The relative admittance $g(x,\Omega)$ as a function of spatial coordinate x/L for $\Omega=\Omega_0$ (the solid curve is its real part and the dashed curve is its imaginary part).

4. Summary

In summary, we have presented a time-dependent Landauer approach to study the dynamic response of a mesoscopic conductor and demonstrated the frequency dependence of its

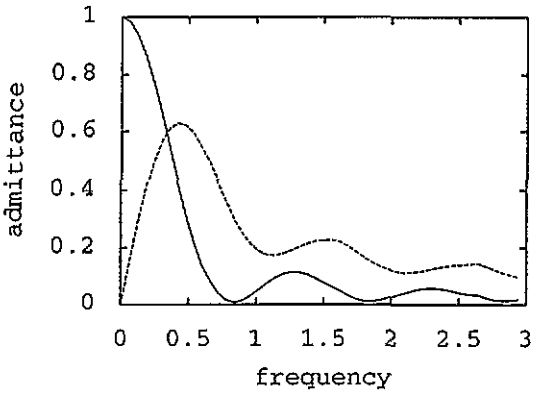

Figure 3. Average relative admittance $\bar{g}(\Omega)$ against Ω/Ω_0. The solid curve is the real part (conductance) and the dashed line is the imaginary part.

admittance. The relevant time scale is found to be the time for an electron to traverse the dissipationless conducting wire between the reservoirs which leads to a characteristic frequency $\Omega_0 = 2\pi v_g/L$ with v_g, the group velocity of the electron in the channel and L, the effective length of the channel. When the bias frequency exceeds Ω_0, the average admittance falls below its DC limit and spatial variations start to appear on a scale $l_\Omega = v_g/\Omega$. Although only a single-channel two-probe model is considered in the present work, the conclusion we draw here should also hold for the more general two-probe systems. Moreover, this work can also be generalized to include the displacement current which, at high frequencies, may yield a contribution to the total measured circuit current comparable to the intrinsic part fully discussed here. Finally, the present study is based on the assumption that the reservoirs respond to the signal electric field immediately. This naturally imposes an upper restriction on the frequency given by the inverse of the reservoir dissipation time which is typically around 10 THz.

Acknowledgments

We thank Professor C S Ting for helpful discussions. We also thank Dr R Landauer and Dr P J Price for their valuable comments. This work is partially supported through a grant from the Office of Naval Research.

References

[1] Landauer R 1988 *IBM J. Res. Rev.* **32** 306
[2] Beenaker C W J and van Houten H 1991 *Solid State Physics* ed H Erhenreich and D Turnbull (San Diego, CA: Academic) Vol 44
[3] Landauer R 1957 *IBM J. Res. Dev.* **1** 223; 1970 *Phil. Mag.* **21** 863
[4] Büttiker M 1986 *Phys. Rev. Lett.* **57** 1761; 1988 *Phys. Rev.* B **38** 9375
[5] van Wees B J *et al* 1988 *Phys. Rev. Lett.* **60** 848
[6] Wharam D A *et al* 1988 *J. Phys. C: Solid State Phys.* **21** L209
[7] Chang L L and Esaki L 1992 *Phys. Today* **45** 36
[8] Gering J M *et al* 1987 *J. Appl. Phys.* **61** 271
[9] Brown E A, Parker C D and Sollner T C L G 1989 *Appl. Phys. Lett.* **54** 934
[10] Frensley W R 1988 *Superlatt. Microstruct.* **4** 497

[11] Jacoboni C and Price P J 1990 *Solid State Commun.* **75** 193; 1991 *Resonant Tunneling in Semiconductors* ed L L Chang *et al* (New York: Plenum); 1993 *Phys. Rev. Lett.* **71** 464
[12] Chen L Y and Ting C S 1990 *Phys. Rev. Lett.* **64** 3159; 1990 *Phys. Rev.* B **43** 2097
[13] Runge E and Ehrenreich H 1992 *Phys. Rev.* B **45** 9145
[14] Fu Y and Dudley S C 1993 *Phys. Rev. Lett.* **70** 65
[15] Büttiker M, Prêtre A and Thomas H 1993 *Phys. Rev. Lett.* **70** 4114
Büttiker M and Thomas H 1992 *Quantum-Effect Physics, Electronics and Applications (IOP Conf. Proc. 127)* ed K Ismail *et al* (Bristol: Institute of Physics)
[16] Landauer R 1992 *Phys. Scr.* **42** 110
[17] Glazman L I *et al* 1988 *Pis'ma Zh. Teor. Fiz.* **48** 218 (Engl. Transl. 1988 *JETP Lett.* **48** 238)
Yacoby A and Imry Y 1990 *Phys. Rev.* B **41** 5341
[18] This is equivalent to neglecting the spreading of the wave packet in the channel region.
[19] Kadanoff L and Baym G 1962 *Quantum Statistical Mechanics* (New York: Benjamin)
Keldysh L V 1964 *Zh. Eksp. Teor. Fiz.* **47** 1515
For its path integral formulation, see
Chou K C *et al* 1985 *Phys. Rep.* **118** 1